Links between soil moisture and InSAR data on a temperate raised peatland subjected to a wildfire

Alexis Hrysiewicz[1,2,*], Eoghan P. Holohan[1,2], Shane Donohue[1,3] and Hugh Cushnan[4]

[1]Irish Centre for Research in Applied Geosciences (iCRAG), University College Dublin, Belfield, Dublin 4, Ireland

[2] UCD School of Earth Sciences, University College Dublin, Belflied, Dublin 4, Ireland

[3] UCD School of Civil Engineering, University College Dublin, Belflied, Dublin 4, Ireland

[4] RPS Group, Elmwood House, 74 Boucher Road, Belfast, BT12 6RZ Northern Ireland, United Kingdom

Corresponding author: Alexis Hrysiewicz (alexis.hrysiewicz@ucd.ie)

Links between soil moisture and InSAR data on a temperate raised peatland subjected to a wildfire

Alexis Hrysiewicz[1,2,*], Eoghan P. Holohan[1,2], Shane Donohue[1,3] and Hugh Cushnan[4]

[1]Irish Centre for Research in Applied Geosciences (iCRAG), University College Dublin, Belfield, Dublin 4, Ireland

[2] UCD School of Earth Sciences, University College Dublin, Belflied, Dublin 4, Ireland

[3] UCD School of Civil Engineering, University College Dublin, Belflied, Dublin 4, Ireland

[4] RPS Group, Elmwood House, 74 Boucher Road, Belfast, BT12 6RZ Northern Ireland, United Kingdom

Corresponding author: Alexis Hrysiewicz (alexis.hrysiewicz@ucd.ie)

Highlights

- InSAR time-series analysis for measurement of ground motion on a raised peatland.
- InSAR is critically influenced by soil moisture changes and temporal baselines.
- Short-term coherence (< 1 year) is mainly controlled by soil moisture changes.
- A wildfire on the raised peatland caused little perturbance of InSAR measurements.
- Backscatter intensity and InSAR phase represent different parts of the peat column.

Abstract

Interferometry of Synthetic Aperture Radar (InSAR) can potentially contribute to the cost-effective regional or global monitoring of the degradation and restoration of peatlands. However, there are uncertainties about the links between InSAR results and peatland ecohydrological parameters, especially soil moisture. Here, we analyse the relationships between the temporal evolutions of InSAR coherence, ground displacements, and in-situ soil moisture measurements for a temperate raised bog at Ballynafagh, Co. Kildare, Ireland, in the period 2017-mid-2021. We also investigate the effects of a wildfire in June-July 2019 on those relationships. InSAR-derived ground displacements from Sentinel-1 C-band radar data indicate long-term subsidence of the intact and Active Raised Bog. Superimposed on the long-term displacement trends are annual oscillations that are linked to variations in rainfall and temperature and that are in phase with changes in soil moisture. We show that InSAR coherence is directly related to the change in soil moisture, with large changes causing coherence decrease or loss. The wildfire removed a 10-20 cm thick mossy vegetation layer across 60-70 % of the intact bog area. The radar backscatter intensity increased after the wildfire, but the InSAR coherence, the InSAR-derived surface displacements and the soil moisture were not noticeably affected. We therefore infer that C-band radar waves attenuate in the active vegetation layer, but penetrate through it into the upper few 10's of cm of the underlying peat. The radar backscatter occurs primarily at this level in the peat, where its coherence is controlled by the soil moisture. These findings underpin application and interpretation of radar for monitoring of peatlands, even if affected by wildfires, which are forecast to increase in both frequency and intensity due to global warming.

1. Introduction

Peatlands are one of the largest carbon sinks on Earth: an estimated 20-30 % of global soil carbon is to be stored in peat, despite fens and bogs covering only a small percentage of the world's land surface (Drösler et al., 2008; Gorham, 1991; Köchy et al., 2015; Renou-Wilson et al., 2019; Yu et al., 2010). However, the role of peatlands in greenhouse-gas (GHG) emissions on global emissions is still unknown or poorly quantified, and so closing this knowledge gap has been become a priority in the context of mitigating global warming (Hiraishi et al., 2014; Leifeld & Menichetti, 2018; Roulet, 2000). In addition, peatland restoration is a focus of current mitigation efforts, (Renou-Wilson et al., 2019), both to maintain the capacity of peatland to be GHG sinks, and also to preserve their endemic flora and fauna, (Parish et al., 2008). Peatlands have been monitored traditionally through in-situ measurements of various key ecohydrological parameters, (e.g., ground level, soil moisture, temperature, groundwater levels, water balance, etc.) and GHG emissions. However, our ability to extend such monitoring of peatlands to regional, national or global scales is a challenge. In Ireland, for example, approximately 15 % of the island – c. 12,700 out of 84,400 km ^{2} - is covered by peat soils (Connolly & Holden, 2009). Globally, 2.84 % of the world land area, amounting to 4.23 million km^2, is peatland (Xu et al., 2018).

Spatial remote sensing has complemented in-situ measurements, providing quantification of peatlands over large areas for several years, (e.g., Connolly & Holden, 2009; Connolly et al., 2007; Jones et al., 2009). Satellite data allow estimates of many ecohydrological parameters to be processed, with worldwide coverage, high accuracy and low cost (data being increasingly open-source and free of charge to end-user), (Lees et al., 2018). For example, methods using the backscatter intensity of synthetic aperture radar (SAR) have been developed to estimate soil moisture at medium spatial resolutions (~1 km), (e.g., Balenzano et al., 2012; Balenzano et al., 2021; Paloscia et al., 2013; Peng et al., 2021; Wagner et al., 2013), and have been generalised to peat soil parameters, (Asmuß et al., 2018; Bechtold et al., 2018; Kim et al., 2017; Millard & Richardson, 2018; Millard et al., 2018; Takada et al., 2009). In recent years, Interferometric Synthetic Aperture Radar (InSAR) has been used to estimate peat surface displacements, (Alshammari et al., 2020; Fiaschi et al., 2019), which are known to be linked to peatland ecohydrological conditions, (Regan et al., 2019). For tropical peatlands, this has led to newly proposed methods for estimating GHG emissions on very large scales from InSAR data, (Hoyt et al., 2020; Zhou, 2013; Zhou et al., 2016).

Ostensibly, peatlands are an unusual target for the successful use of InSAR time-series methods to derive surface displacement. Vegetated target areas are prone to strong decorrelation of the radar phase over successive radar acquisitions, (Zebker & Villasenor, 1992). This is especially problematic at shorter radar wavelengths (e.g. X-band or C-band), for which penetration of the vegetation by the radar waves is progressively inhibited. Decorrelation in such areas is linked to transient backscattering conditions in the vegetation and/or to variations in underlying soil properties, especially soil moisture (Nesti et al., 1995). Peatlands such as raised bogs or blanket bogs are characterised by a relatively thin (5-50 cm) active vegetation layer, referred as the acrotelm, which when in good condition is dominated by sphagnum mosses. Such vegetation could present more stable backscattering dynamics than other vegetation types (e.g. grasslands), and thus be a factor in the unusually high coherence at peatlands. On the other hand, coherence at peatlands has been noted to decline during seasonal dry periods as the groundwater table declines (Tampuu et al., 2020). Thus soil moisture could exert a complementary or overriding control on coherence, but links between in-situ soil moisture measurements and InSAR data have been lacking.

A further complication is that peatlands can be affected by wildfires. Depending on burn duration and intensity, wildfires can cause significant damage to both the active vegetation and the underlying peat, (Wilkinson et al., 2020). In this case, wildfires can potentially change a peatland's ecohydrological state and its ability to sequester carbon (Kettridge et al., 2012; Reddy et al., 2015). For example, Hooijer et al. (2014) defines different relationships between GHG emissions and peatland surface displacements depending on peat conditions (burnt, drained, etc.). Khakim et al. (2020) also shows an increase in peatland subsidence after severe wildfire on tropical peatlands. Understanding of the impact of wildfire on InSAR results for peatlands is thus important for both application and interpretation, but to date has received little if any attention.

In this study, we analyse C-band satellite InSAR products, including coherence maps, temporal evolutions of displacements and SAR intensity from Sentinel-1 IW data for a temperate raised bog where soil moisture was measured in-situ over the same time period. The occurrence of a large fire on the bog in June-July 2019 presents an opportunity also to understand the effects of wildfire and sudden peatland vegetation loss on the InSAR products such as coherence and displacement. We first introduce the studied peatland and present the spatial observations from remote sensing via both multispectral and SAR data. We then analyse the links between in-situ soil moisture data and the InSAR parameters, as well as their variations due to the fire. Our results provide new insights into the level at which radar backscattering occurs in a temperate raised peatland and into the impacts of wildfire on InSAR in such a setting. Furthermore, these results highlight key elements for time-series InSAR computation on peatlands to optimise coherence, which will improve the wider application of this remote sensing method to the study of peatlands.

2. Methods

2.1. Study site

Ballynafagh bog is a temperate raised peatland located in Ireland (Co. Kildare), (see Figure 1). The bog is a Special Area of Conservation (SAC), as defined by the European Union's Habitats Directive (Council Directive 92/43/EEC of 21 May 1922). Regional hydrological data suggest that Ballynafagh Bog SAC receives average precipitation of 785 mm.yr^{-1} (1981-2010), with an estimated evapotranspiration rate of ~ 528 mm.yr^{-1}, leaving an average effective precipitation of 257 mm.yr^{-1}: data from MET Éireann (MET), the Irish meteorological service. With an average elevation of 85 m (a.s.l.), the bog has been geomorphologically classified as a basin bog (Kelly, 1993). It is an Irish midland eastern type raised bog, occurring at the eastern limit of the range of raised bogs in Ireland (Cross, 1990). The area is underlain by muddy Carboniferous limestones, interbedded with calcareous shales. The subsoils are predominantly clay-rich glacial tills.

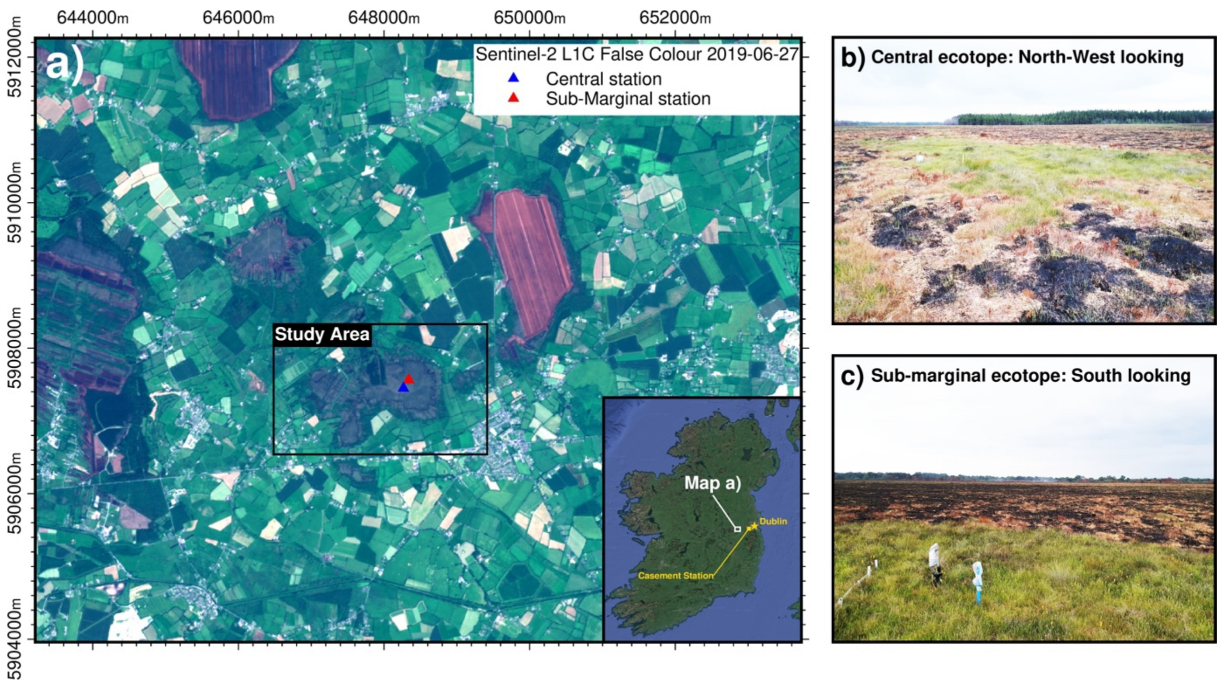

Figure 1: Ballynafagh bog. ***a)*** *The study area and its surroundings in a Sentinel-2 L1C False Colour image acquired on 2019-06-27, a few days before the wildfire. Coordinates in meters for UTM zone 29U. The blue triangle and red triangle mark the locations of the Central and Sub-Marginal monitoring stations, respectively. The inset shows the location of the study area in Ireland (from Google Earth images).* ***b)*** *Post-fire field image, taken on 2019-07-19, of the area around the Central monitoring station.* ***c)*** *A post-fire field image, taken on 2019-07-19, of the Sub-marginal monitoring station.*

Nearly half the original bog extent within the SAC has been subject to cutting and harvesting of peat in historical times. The uncut high bog has an area of 70 ha and a cutover area of 90 ha. Large drains were installed across the bog throughout the past century for both manual and mechanical peat extraction. Although peat cutting no longer occurs on this site (ceased approximately 2010), no physical restoration measures have been carried out on site. In addition, a significant proportion of the bog was damaged by fire during the mid-1990's.

Field mapping in 2013, following the classification of Kelly and Schouten (2002), sub-divided the bog surface into several ecotopes (Figure 2 a). These are areas of similar vegetation type, ecological condition and microtopography, (Fernandez et al., 2014; Kelly & Schouten, 2002). The ecotopes are named Central, Sub-central, Sub-marginal and Marginal, in order of decreasing prevalence of sphagnum mosses and increasing prevalence of heathers and other bushy vegetation. The sphagnum-dominated Central and Sub-central ecotopes represent areas of Active Raised Bog (Fernandez et al., 2014), i.e. bog that "still supports significant areas of vegetation which are normally peat forming". These ARB areas, with a net accumulation of peat, covers 6.48 ha (9.25 %) of the uncut (high) bog area, while the remaining 63.58 ha (90.75 %) of the high bog area consists of non-peat accumulating ecotopes. A Pinus Contorta plantation occurs in the North-West of the bog, which occupies 10.02 ha (20 %) of the high bog area and forms a semi-open canopy. The Face Bank ecotope corresponds to

148 the edge of the high bog where recent cutting has occurred and is characterised by a sharp surface

149 gradient from the high bog to the adjacent lower-lying area of cut-over peat.

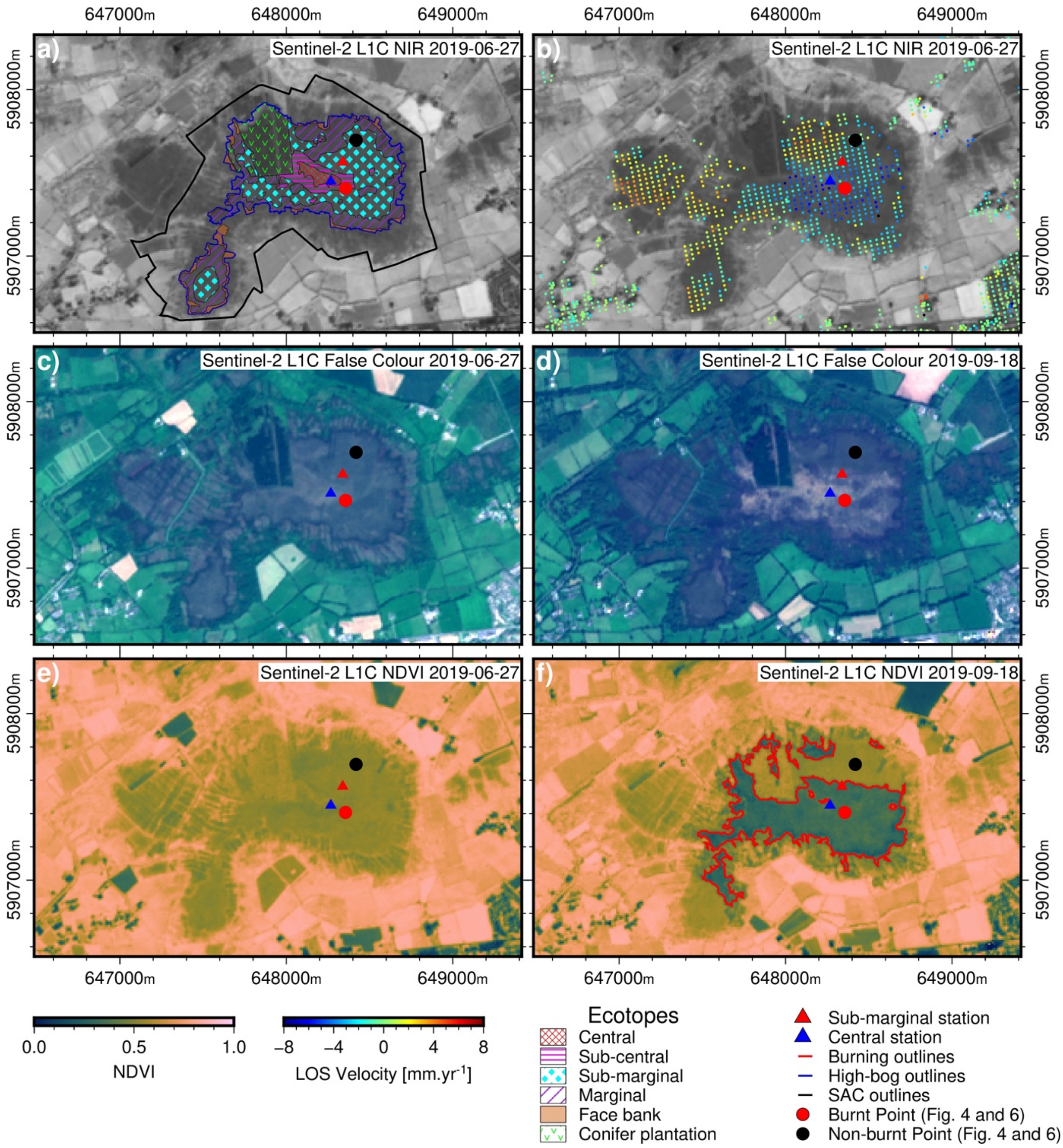

150

Figure 2: Maps of ecotope and remote sensing data for Ballynafagh bog. ***a)*** *Ecotopes of Ballynafagh bog with the NIR Sentinel-2 L1C image on 2019-06-27 as background;* ***b)*** *InSAR estimate of peatland surface*

displacements rates in satellite LOS for the period 2017-2021 with NIR Sentinel-2 L1C image on 2019-06-27 as background; ***c)-d)*** *Sentinel-2 L1C false colour images acquired before (on 2019-06-27) and after (on 2019-09-18) the wildfire in July 2019. Spectral bands are Red: 665 nm, Green: 560 nm, Blue: 490 nm;* ***e)-f)*** *NDVI from Sentinel-2 L1C images acquired on 2019-06-27 and 2019-09-18 (655 nm and 842 nm), with the outline of burnt areas in red. Coordinates are in meters for UTM zone 29U.*

2.2. In-situ monitoring data

Two soil moisture monitoring stations were installed in the high bog at Ballynafagh in 2017 (Figure 1). The sensors are METER GS3's which measure the dielectric permittivity, and by calibration, the soil moisture of the medium in which the sensor is installed. The sensors were planted at 15 cm depth below the peat surface, following excavation of a shallow hole, which was subsequently back filled using the excavated material. The sensors were installed in Central and Sub-marginal ecotopes on the high bog. They were logged using METER EM50 data loggers from 2017 to 2020, and subsequently using METER ZL6 data loggers. The change in data logger type was made to reduce the possibility of power loss, as occurred on a few occasions in 2018 and 2019. The ZL6 data loggers are solar powered and, since their installation, data has been continuously monitored every 30 minutes. In addition, a piezometer pinned to 1.5 m-depth (with 0.5 m screen) was installed at the Sub-marginal station in March 2019 and functioned with a continuous logging of water table depth until end of October 2020, (sensor: HYDROS 21; logger: METER ZL6).

A post-fire inspection on the 19th of July 2019 revealed that the two monitoring stations had escaped any significant damage by the wildfire. The Central station was located at the southern extremity of a c. 20 m by 10 m "island" of preserved or lightly damaged vegetation (Figure 1 b). The Sub-marginal station was located within the domain of intact vegetation a few metres from the border of main burn area (Figure 1 c). Where impacted, the fire resulted in the removal of almost all surface vegetation on the high bog. It was noted, however, that although the bog surface appeared completely scorched, the fire did not appear to affect the peat below 3-5 cm depth.

Time series of daily and hourly precipitation, soil temperature (to 10 cm depth), potential evapotranspiration and evaporation are provided by MET Éireann for the Casement station (Lat. 53.303 and Lon. -6.437). This station is twenty kilometres from Ballynafagh bog. Other meteorological stations are closer to the bog, but these record only daily precipitation and atmospheric temperature, whereas Casement station records data hourly and monitors the full range of soil parameters. Since the temperature and precipitation data from Casement station and from the MET stations closest to Ballynafagh bog are very similar (see Supplementary Material), we use the Casement data as a proxy for the local meteorological and soil conditions for the area around Ballynafagh bog.

2.3. SAR data processing

During a SAR acquisition, the satellite emits radar waves that reflect (backscatter) off ground targets and the same satellite measures the return waves. The result is an image containing a complex number in each pixel in radar geometry. The modulus of the complex image (with a normalisation of pixel size - topography) and represents the power of the backscattered signal and is termed the intensity. The argument of the complex image is termed the phase and is related to: (1) the propagation time of the radar waves between the satellite and the ground; (2) the pixel phase, related to the geometry and dielectric properties of the ground targets.

The phase information within a single image is not usable because of spatial randomness of the pixel phase, but the difference of phases within two SAR images of the same target area can be calculated to obtain the changes in propagation time. In this case, the phase difference is directly linked to any ground surface displacement that occurred between the two image acquisition dates, as well as to other contributions from topography, satellite orbits, changes in atmospheric conditions, noise, etc. The image obtained by phase differencing is called an interferogram. The stability (i.e. similarity) of the pixel phases between the two SAR acquisitions is termed the coherence (Zebker & Villasenor, 1992). Loss of coherence can be called decorrelation.

The InSAR method for calculating surface displacements consists of firstly accurately repositioning the one image with respect to the other image (coregistration), and then subtracting or minimising the contributions of all the other sources of phase variation, especially topography and atmosphere (Massonnet & Feigl, 1998). The resultant image is termed a differential interferogram, and hence the method is commonly termed D-InSAR. To obtain the time series of surface displacements - i.e., the evolution of displacements for consecutive SAR acquisitions - an inversion can be done upon a network of differential interferograms. The interferograms can computed either relative to one reference image (single reference network) or relative to several reference dates (multi-reference network) (e.g., Casu et al., 2006; Ferretti et al., 2001). The time elapsed between the acquisitions of the SAR images used to generate each interferogram is termed the temporal baseline. A good network design usually minimises the temporal baselines to maximise coherence (i.e. minimise temporal decorrelation).

For this study, InSAR coherence and displacement estimations were derived by processing the Sentinel-1 Single Look Complex (SLC) images acquired in Interferometric Wide Swath mode (IW) in Ascending pass. All available acquisitions between 4th January, 2017 and 18th June 2021 (~4.5 years) were used. Images acquired during periods of light snow cover are included in the dataset, but any effects on the results from snow cover are within noise. The coregistration was performed by using the GAMMA® software and the Shuttle Radar Topography Mission (SRTM) Digital Elevation Model (DEM), (Farr et al., 2007; Scheiber & Moreira, 2000; Wegmüller et al., 2015; Wegnüller et al., 2016).

From our coregistered SLC stack, the conversion of radar phase to displacement was achieved by using the GAMMA Interferometric Point Target Approach (IPTA) with a multi-reference network of interferograms, which included both single-look and 10/2 multi-look images (kernel-based image averaging to increase signal-to-noise ratio at lower spatial resolution), (Werner et al., 2003). The interferogram network for displacement estimation was created as follows: if N is the index of a SAR acquisition, all N-1, N-2, N-3 interferograms are used together with the N-3 months and N-1 year interferograms, (see Supplementary material). In parallel, coherence maps were computed by using a 10 pixels/2 pixels multi-look (same windows as used in IPTA approach) and a 5 pixels/5 pixels estimation kernel (in Radar geometry). Geocoding of images was done with a spatial resolution compatible with the SAR resolution (~ 30 metres). To investigate the variation of coherence around the two in-situ monitoring stations, we used the same estimation parameters, regarding the multi-look kernel and kernel for estimating the coherence, and the coherence was filtered by using a mean kernel of 3 pixels/3 pixels, centred on the pixels containing each station. Thus the coherence around each in-situ stations represents an average value for a ground area of dimension ~ 75 x 125 m.

2.4. Multispectral data processing

To map fire-related vegetation changes at Ballynafagh, we used Sentinel-2 multispectral images at L1C level (without atmospheric correction on radiance measurements) that were acquired before and after the wildfire event. The multispectral bands were cropped and False-Colour, NDVI and IR images were created (band combinations are given in the caption to Figure 2). Without changing the coordinate reference system, the spatial resolution of the optical images is 10 metres. From the post-fire NDVI image, we extract the outlines of burnt areas by using segmentation with a minimum threshold of NDVI = 0.2 and a maximum threshold of NDVI = 0.4. Only burnt areas with an area of at least 25 pixels and non-burnt areas of a minimum of 5 pixels (respecting 4-connected pixels) are selected.

3. Results

3.1. InSAR-derived surface motion velocities

Figure 2 b shows the estimated linear velocity of peatland surface motion over the 4.5-year observation period. Each coloured point corresponds to a pixel that displays suitably high coherence and low phase uncertainty throughout the observation period. Overall, point coverage is good across the high bog area, especially in the sphagnum-dominated or sphagnum-rich ecotopes (Central, Sub-central and Sub-marginal). Point retrieval is more challenging in the much of the areas of marginal ecotope, face bank and the cut-over peat. Based on the expected vertical motions for this target, and a conversion factor of 1.3, we can transform the Line of Sight (LOS) displacement to vertical displacements, such that a negative value implies subsidence, and a positive value implies uplift. In general, we consider an absolute velocity of more than 1 $mm.yr^{-1}$ to be significant (Fiaschi et al., 2019).

The InSAR velocity data indicate that during the observation period most of the high bog area, straddling the Central, Sub-central, and Sub-marginal ecotopes, has undergone subsidence at average rates of up to -9 $mm.yr^{-1}$. Several other areas within and just outside the SAC boundary are apparently affected by uplift at average rates of up to +5 $mm.yr^{-1}$. These areas include a northern part of the high bog classified mainly as Marginal ecotope, as well as zones of cut-over (i.e., harvested) bog to the west. The obtained InSAR-derived velocities are thus dichotomous and somewhat heterogenous, but they overall display a broad consistency in space across the bog.

3.2. RGB and NDVI mapping of the wildfire-affected areas

Sentinel-2 L1C False Colour images with minimal cloud coverage (and similar colour dynamics) show that the burnt areas in the central part of the bog are identifiable by lighter colours in the post-fire image (Figure 2 c-d). By comparing these maps with Figure 1 b-c, we can also see that the Central station is surrounded (preserved on its "island") by burning and that the Sub-marginal station is located at the edge of the burnt area. Furthermore, the NDVI images (c.f., Figure 2 e-f) allow a more precise delimitation of the burnt areas: the NDVI there decreases from a pre-fire value of $0.53\pm0.03(1\sigma)$ to a post-fire value of $0.33\pm0.04(1\sigma)$. In other areas that from field inspection were demonstrably unaffected by the fire, such as the northern part of the high bog (NDVI > 0.5), little or no change in NDVI occurs between the pre-fire and post-fire images. The red contours on Figure 2 d represent the boundaries of areas affect by the fire as derived from the NDVI thresholds. These contours collectively encompass an area of 0.47 km^2, which means that about 60-70 % of the high bog area has been affected and damaged by the wildfire.

From other RGB, IR and NDVI images in the Sentinel-2 time series (see Supplementary Materials), we estimate that the wildfire began after 30th June, 2019 and reached its final extent by 7th July, 2019. We are not able to identify the start and end dates of the fire more precisely from the Sentinel-2 data because of cloud cover in many of the multispectral images. Field observations confirm that the wildfire had stopped burning sometime before 19th July, 2019.

3.3. Temporal relations between in-situ soil parameters and InSAR-derived displacements

The time series of peat surface displacements around the Central and Sub-marginal in-situ monitoring stations (average radius of 25 m) show long-term linear subsidence trends, of -3.7±0.2(1σ) mm.yr^{-1} and -1.5±0.2(1σ) mm.yr^{-1}, respectively (Figure 3 a-b). Superimposed on these long-term trends are roughly annual oscillations in surface displacement of up to ±10 mm. Maximum uplift typically occurs between January-March (winter), whereas maximum subsidence typically occurs in June-August (summer).

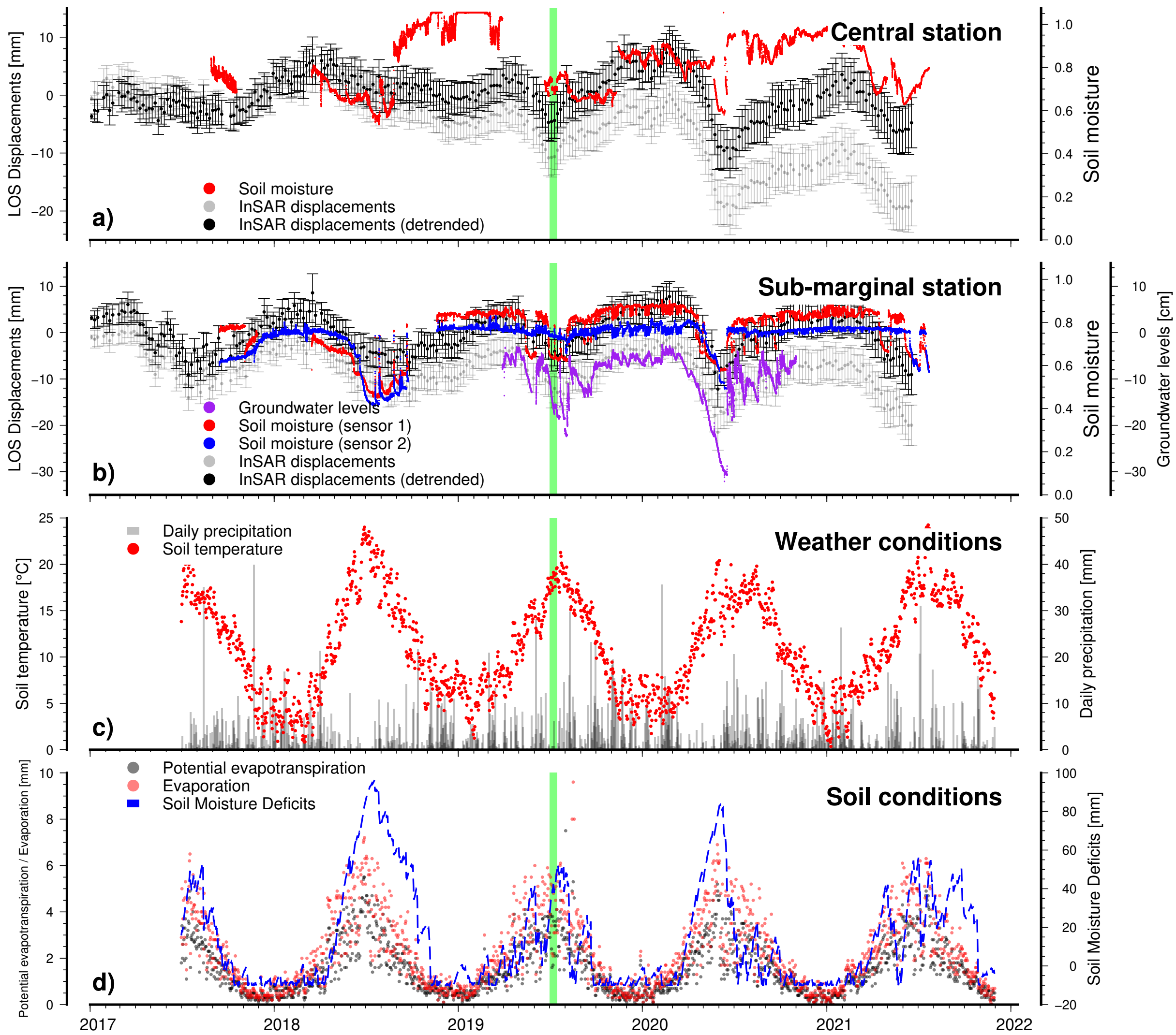

Figure 3: Time series of in-situ and remotely-sensed parameters. ***a)-b)*** *Temporal evolutions of LOS displacements, soil moisture for the Central station (in* ***a)****) and the Sub-marginal station (in* ***b)****), with the groundwater levels.* ***c)*** *Temporal evolutions of rain precipitation and soil temperature for Casement MET station (Lat. 53.303 and Lon. -6.437) located 22 km from Ballynafagh bog;* ***d)*** *Temporal evolutions of potential evapotranspiration, evaporation, and soil moisture deficits (calculated by using a 'poorly drained' model) for Casement MET station. The estimated duration of the 2019 wildfire event is displayed as a green bar.*

The temporal evolution InSAR-estimated surface displacement at Ballynafagh bog closely tracks the temporal evolution of soil moisture and groundwater levels measured in-situ (Figure 3 a-b). Soil moisture is highest – typically at saturation (or at sensor detection limit) – during the winter and early spring months. Soil moisture decreases to its lowest values during the summer months. Average groundwater level at the Sub-marginal station is 8 cm below the ground surface, (see Figure 3 b). In winter, the groundwater levels reach up 4 cm below the ground surface, and declines up to 32 cm in summer. Groundwater and soil moisture changes are positively correlated in time. Also the InSAR-derived displacements are near synchronous with both groundwater and soil moisture variations. Although the timescale of seasonal soil moisture and groundwater level decreases is similar to the timescale of seasonal subsidence estimated from InSAR, the recovery of soil moisture and groundwater to high levels is much sharper – i.e. occurs over a much shorter timescale – than the seasonal upswing in surface displacement. Finally, the magnitudes of changes in groundwater and ground surface levels are in ratio of 10:1.

The seasonal variations of in-situ soil moisture and InSAR-estimated surface displacement at Ballynafagh bog closely track the meteorological data and soil condition estimates at the regional Casement MET station. The largest amplitudes of surface oscillations at both of the Ballynafagh stations are coincident with periods of low to no rainfall for several weeks (i.e. drought conditions) in Summer 2018 and Summer 2020 (Figure 3 c). These drought periods were characterised by comparably long periods of elevated soil temperatures (Figure 3 c), as well as correspondingly high estimates of evaporation, evapotranspiration and soil moisture deficits (Figure 3 d).

The period of the wildfire in 2019 (green bar in Figure 3) is coincident with a period of low soil moisture at Ballynafagh bog (Figure 3 a-b). A sharp decrease in soil moisture (0.8 to 0.7 over 4-5 days) can be noted at the Sub-marginal station just before the wildfire. The wildfire occurs also near the summer peak of temperature and a period of rapidly increasing soils moisture deficits as estimated at the regional Casement MET station. It is worth noting that the summer of 2019 was not the warmest or driest in the period from 2017-2021. Ostensibly, conditions may have been more favourable for wildfires in 2018 and 2020, but ignition did not occur.

3.4. Evolution of SAR intensity and InSAR displacement for burned and non-burned areas

Since areas immediately around the monitoring stations seems to have undergone partial burning, we here show data for two areas within the same ecotope (sub-marginal) located further inside the burned and non-burned areas of the peatland. The purpose is to test for contrast in the behaviour of the SAR and InSAR data in the burned and non-burned areas. Data within a 50-m radius of a point in the burnt area (red point in Figure 2) and a point in the non-burnt area (black point in Figure 2) are shown in Figure 4.

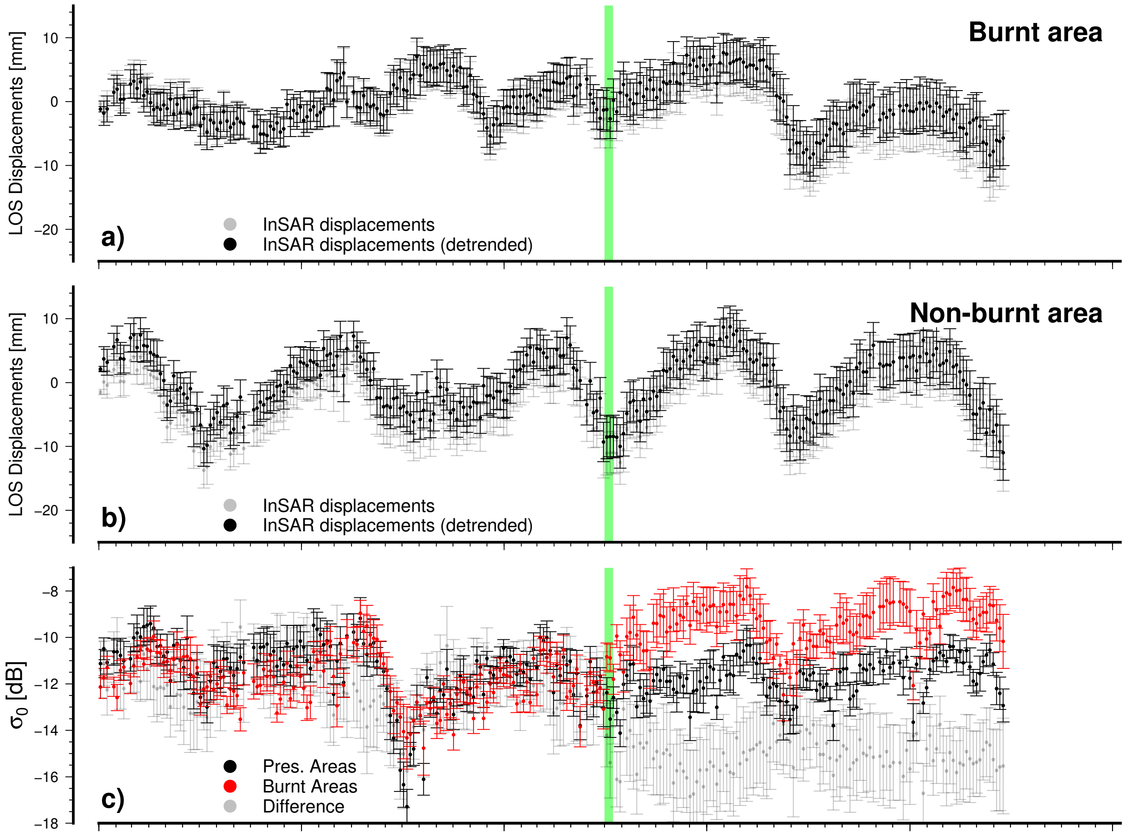

Figure 4: Time series of SAR intensity and displacement for the burnt and non-burnt areas. ***a)-b)*** *Temporal evolutions of LOS displacements for burnt area (in* ***a)****) and non-burnt area (in* ***b)****).* ***c)*** *Temporal evolution of SAR intensity for burnt and non-burnt areas. The estimated duration of the 2019 wildfire event is displayed as a green bar.*

The InSAR displacement time series for both points located show no clear effect due to the wildfire (Figure 4 a-b). The long-term absolute velocities appear to be lower at these points than those observed at the in-situ stations (-0.9±0.2(1σ) mm.yr^{-1} and -0.4±0.2(1σ) mm.yr^{-1} respectively), while the annual oscillations are very similar (Figure 3). The variations in long-term velocity and in the magnitude of annual oscillations further show that the InSAR-derived displacements are dichotomous and heterogenous within the bog. However there is no shift or variation in the burnt area displacement time series that is coincident with the wildfire.

On the other hand, the temporal evolutions of the mean SAR backscatter intensity (σ_0) for the burnt and non-burnt areas differ significantly after the wildfire (Figure 4 c). Before the fire, the intensity evolutions of both areas are very similar. After the wildfire period, the relative magnitudes of the annual SAR intensity fluctuations remain equal for both burned and non-burned areas. The SAR intensity of the burnt areas increases overall, however, and it becomes consistently about 2-3 dB higher than that of the preserved areas.

3.5. Evolution of InSAR Coherence

Figure 5 shows the changes in coherence over Ballynafagh bog in the days before and after the wildfire. Overall, the coherence on the bog is high to moderately high for the temporal baselines considered here. There is not a systematic pattern of spatial or temporal change in the coherence that one can relate to the wildfire. The maps with lowest coherence are formed when one SAR image of the pair was acquired on a rainy day – for example, the coherence maps spanning June 23rd - July 5th, June 23rd - July11th, July 23rd - August 4th and July 29th - August 4th. Low coherence thus appears to be simultaneous with differences in precipitation, in groundwater levels, and hence differences in soil moisture, between the pair of SAR image acquisitions. Conversely, high coherence is associated with similar precipitation and soil moisture conditions for the SAR acquisition pair.

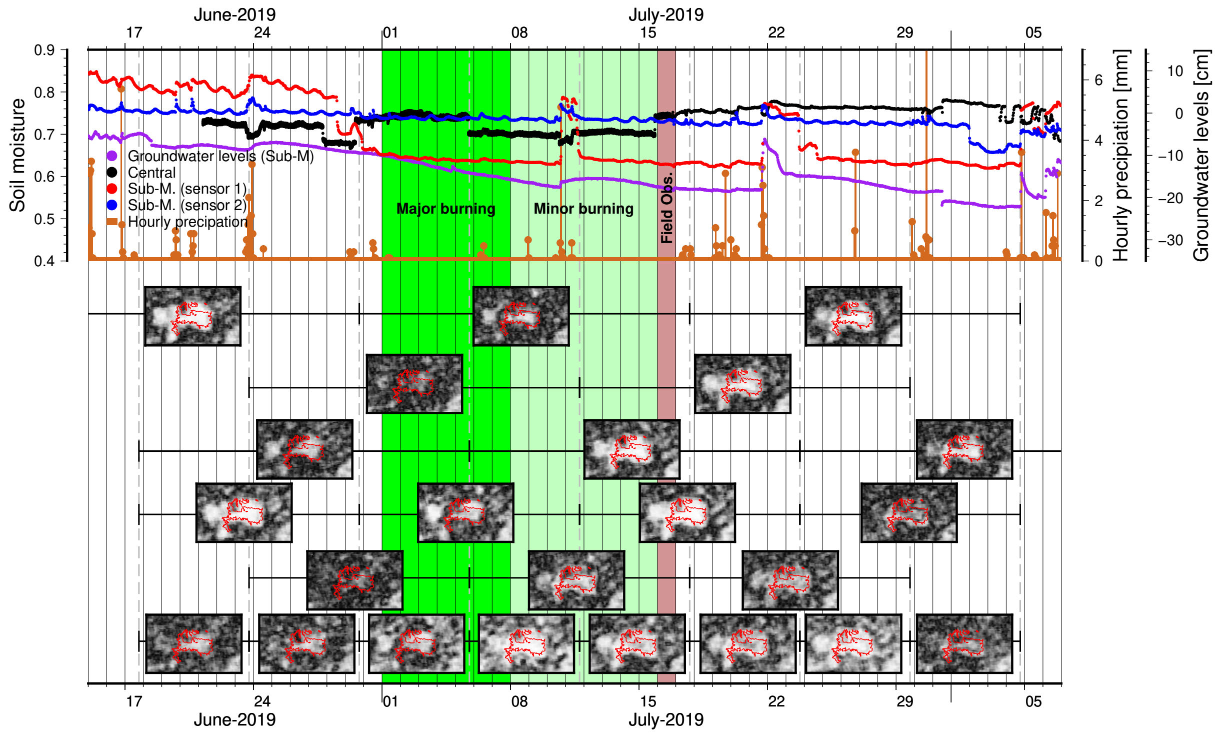

Figure 5: Timeline of InSAR coherence maps and soil moisture at Ballynafagh Bog. The upper section shows the temporal evolutions of soil moisture, and groundwater levels as measured at Ballynafagh Bog and hourly precipitation as measured at the Casement MET station. The lower section shows coherence maps for pairs of SAR images, the acquisition dates of which are given by the bars either side of each coherence map. The rows of coherence maps are arranged from top to bottom in order of decreased temporal baseline. In the greyscale coherence maps, black is low coherence and white is high coherence. The red contour is the outline of the areas affected by the wildfire.

To illustrate the variation of coherence with soil moisture over the entire observation period, we show a coherence matrix for the areas immediately around both monitoring stations (Figure 6 a). Each point in this matrix represents the coherence in each pair of images in the stack at the Central (upper left) or Sub-marginal (lower right) monitoring stations. The image acquisition dates for the pair are given on the horizontal and vertical axes. We make three main observations from the matrix.

350

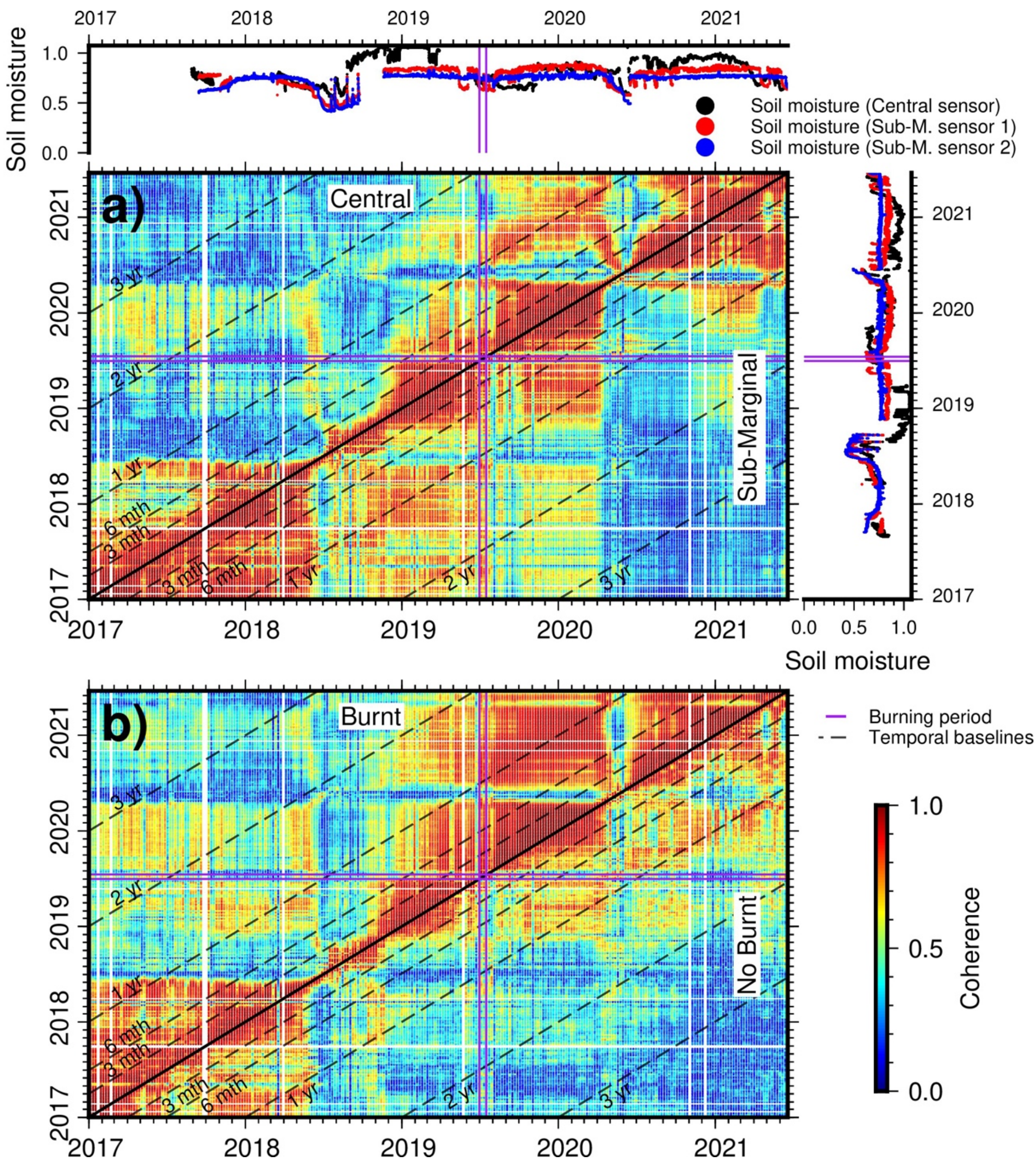

351

*Figure 6: Matrix of coherence for all possible SAR image pairs during the observation period **a)** for the in-situ monitoring stations in Ballynafagh bog and **b)** for the burnt and non-burnt areas as described in Figure 4. For the part **a)**, the upper left triangle of the matrix represents coherence values for the area immediately*

around the station in the Central ecotope. The lower right triangle, on the other side of the solid black diagonal line, represents values for the area around the station in the Sub-marginal ecotope. For the part ***b)****, there is a similar layout for the burnt and the non-burnt areas. The matrix plot axes give the acquisition dates of the two SAR images in each pair. The dashed black lines are isochrons that represent where the temporal baselines of image pairs. For comparison to the temporal evolution of the coherence, the temporal evolution of in-situ soil moisture at both stations is displayed on the plots alongside the matrix in part* ***a)****. The purple lines crossing the matrix and the plots mark the start and end of the wildfire. Overall, as expected, coherence decreases with increased temporal baseline. For a given temporal baseline, however, coherence is higher when soil moisture conditions are similar for each acquisition in an image pair, and coherence is lower when soil moisture conditions differ substantially.*

Firstly, coherence decreases as the temporal baseline of the image pair increases. This is a consequence of temporal decorrelation and is typical of vegetated target areas. This is the main factor controlling coherence on the long term. Secondly, there are abrupt decreases in coherence associated with large differences in soil moisture. These soil moisture-related coherence decreases are superimposed on the background trend of decreased coherence with increased temporal baseline. Coherence loss due to soil moisture difference is particularly pronounced where one SAR image in a pair was acquired during the summers of 2018 or 2020, when large decreases and fluctuations of soil moisture occurred during drought conditions. Under these drought conditions, high coherence (>0.7) interferograms are formed only from image pairs with a temporal baseline of less than 2-3 weeks. Thirdly and from Figure 6 b, the wildfire does not cause a noticeable instantaneous and short-term perturbation on the observed values of coherence compared to the overriding effects of temporal decorrelation and soil moisture difference. The post-burning coherence of the burnt area seems to become slightly higher for longer temporal baselines (>1 year) compared to that of the non-burnt area, but it is unclear if this is a significant change.

4. Discussion

4.1. Link between displacements and peat soil parameters

Estimated surface displacements, backscatter intensity and in-situ soil moisture at the raised peatland of Ballynafagh all follow similar temporal fluctuations, with an annual periodicity resulting from dry (spring-summer) and wet (autumn-winter) periods. On the raised bogs, in the absence of human interference, the peat-condition is controlled mainly by short-term seasonal and long-term climatic variation (temperature, rainfall and insolation), which control evapotranspiration and water table levels (Heikurainen et al., 1964). Then, groundwater levels are the driving force of soil moisture. In this case, soil moisture can be a proxy of water-table levels and vice versa, (see Figure 3 b).

The long-term displacement trends of subsidence at Ballynafagh bog could be related to internal peat processes, such as peat compaction and oxidation, and potentially to long-term variations in deeper hydrogeological conditions within or under the peatland, (Ewing & Vepraskas, 2006; Regan et al., 2019). It is this long-term part of the displacements that Hooijer et al. (2010), and later Hoyt et al. (2020), propose to use to estimate GHG emissions from InSAR motions on tropical peatlands, (Zhou, 2013; Zhou et al., 2016).

The short-term (i.e., annual) oscillations in displacement are consistent with annual variations of surface elevation that are commonly measured in-situ on raised peatlands elsewhere. These short-term variations of the peatland surface elevation are termed bog or mire ‘breathing’, and they are controlled by annual rise and fall in groundwater levels (Fritz et al., 2008; Howie & Hebda, 2018; Zhou et al., 2010). As such, variations in soil moisture and estimated displacements at Ballynafagh bog are likely to be an expression of short-term (annual) water-table changes.

Backscatter intensity also shows a seasonal variation that closely mimics that of the estimated surface displacement (Figure 4). The simplest interpretation of this relationship is that backscatter intensity is reduced as the water table falls and soil moisture is reduced - especially in the drought periods. This interpretation is supported by previous work demonstrating a strong positive correlation between backscatter intensity and soil moisture (Dobson et al., 1992). However, the more gradual recovery of both displacement and backscatter intensity compared to the sharper recovery of soil moisture suggest that the radar response is governed not only by soil moisture in the upper unsaturated domain of the peat. The slow recovery of intensity and displacement can be attributed to a slow recovery of the groundwater level after the drought periods. Groundwater levels in the active area of healthy raised bogs such as Ballynafagh typically lie at about 8 cm below the ground surface. As demonstrated here, however, they can drop to several 10s of cm below the surface during drought periods. The backscatter from the peat thus seems to be controlled not only by moisture content in the unsaturated uppermost peat but also by the total saturated volume of the upper 10-30 cm of the organic soil. Future work with co-located piezometers and soil moisture sensors at variable depths in the peat could test this hypothesis.

4.2. Implications of soil moisture changes for InSAR computations

An important observation in our study is that the coherence on a raised peatland can increase over time. This compensates for typical temporal decorrelation on longer temporal baselines (> 1-2 years, and, to our knowledge, this is only observable on peat targets for these durations). The coherence oscillates with the annual frequency with respect to the first coherence value. Indeed, the coherence remains high several months after the master acquisition (about 3 months), decreases for durations of about 6 months, then increases 1 year after the first acquisition, and so on (Figure 6). Thus, it is possible to observe medium or high coherence for 1- or even 2-years temporal baselines.

We can easily define that, (after simplifications), (Zhang et al., 2008):

$$\gamma_{\text{Observed}} = \gamma_{\text{Temporal}} \times \gamma_{\text{Soil Moisture}} \times \gamma_{\text{Noise}}, \tag{1}$$

with γ the InSAR coherence. With a coherence of 0.7 on the 1-2-years interferograms and equation 1, we can interpret that γ_{Temporal} is also higher than 0.7, which demonstrates that temporal decorrelation is extremely low on peatlands: probably the lowest compared to other vegetation targets, (Tampuu et al., 2020). In our study case, we show that soil-moisture-related coherence ($\gamma_{\text{Soil Moisture}}$) is the main factor controlling the recovery of coherence on interferograms with long temporal baselines (>1-2 years), (cf. Figure 6).

Conventional and improved InSAR approaches, suitable for peatland applications, are based on interferogram networks selected to minimise temporal and perpendicular baselines, and hence the coherence of the interferogram stack, (e.g., Alshammari et al., 2020; Alshammari et al., 2018; Bateson et al., 2015; Casu et al., 2006; Cigna, Novellino, et al., 2014; Cigna, Sowter, et al., 2014; Hooper, 2008; Sowter et al., 2013; Werner et al., 2003). Figure 7 shows the probability of having a coherence higher than 0.5 with respect to the temporal baselines, for each season when the first acquisition (master acquisition) is acquired and for the Sub-marginal station. Due to the temporal evolution of the soil moisture, we can observe that each season offers different evolutions of the probabilities, with two end-members for the winter and summer seasons. In winter and due to the link between the coherence and the soil moisture change, the probability oscillates are caused by the high stability of the soil moisture with the master date. On the contrary, when soil moisture changes for a short period in summer, the probability of having a high coherence is lower, and more controlled by temporal decorrelation. This is particularly true for interferograms with 6-month temporal baselines for which the probability of having an incoherent interferogram is very high. Thus, the coherence is related to the selection of the master date on peatlands: i.e., it seems more robust to select a master acquisition (or super single master regarding the InSAR correlation) in spring in order to maximise the coherence of the whole stack.

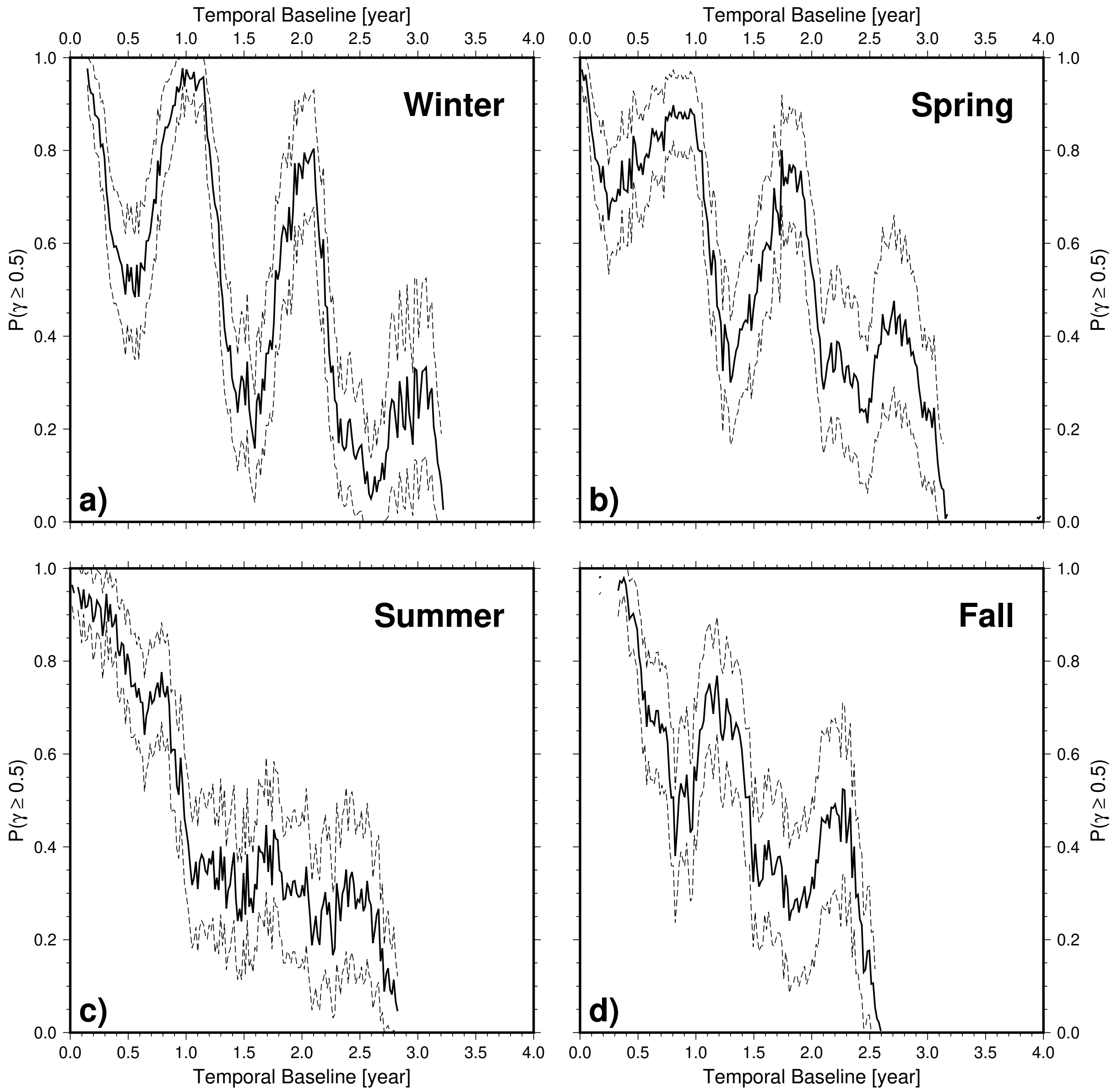

Figure 7: Relations between the probability to have a coherence superior to 0.5 at the Sub-marginal station as a function of temporal baseline, and the season of master acquisition. The dashed lines correspond to 95% confidence levels. The probabilities are estimated using empirical cumulative distribution function (ecdf): $P(\gamma \geq 0.5) = 1 - ecdf(0.5)$.

According to the proposed InSAR phase and coherence models, the InSAR phase should also be modified by soil moisture (e.g., De Zan et al., 2014). However, we are not able to extract this phase due to the peat surface displacements. In addition, we do not observe significative non-zero closure phases in our interferograms for which we have identified changes in soil moisture. This seems expected because the observation of closure phases is defined by our ability to multi-look and filter the SAR/InSAR data, (Eshqi Molan & Lu, 2020b; Molan et al., 2020). In contrast, high residuals of phase are observed during the InSAR processing. These phase residuals map perfectly to the spatial extent of the bog, and they are unrelated to potential atmospheric delay. The InSAR phase in C band that is interpreted as displacement could therefore include part of unobserved soil moisture phase on the peat targets. This could modify the results during the inversion of displacements and cause an underestimation of the amplitudes of the annual oscillations (in the case of peatlands), (Zwieback et al., 2017). Consequently, InSAR-derived displacement should in future be compared with ground-based displacement measurements to estimate artefacts due to soil moisture on InSAR-derived displacements.

4.3. Interpretation of SAR/InSAR products related to soil moisture changes on raised peatland

The relationships between changes in soil moisture (and vegetation) and SAR/InSAR estimates have been well documented since the beginning of the InSAR studies, whether it is SAR intensity, InSAR phase, coherence or closure phase, (e.g., Barrett, 2012; De Zan & Gomba, 2018; De Zan et al., 2014; De Zan et al., 2015; Nesti et al., 1995; Zhang et al., 2008; Zwieback et al., 2015a, 2015b, 2017). However, the wildfire affecting Ballynafagh bog provides an opportunity to further identify the physical meaning of the SAR/InSAR estimates.

Our results for Ballynafagh bog demonstrate that SAR backscatter intensity should be carefully interpreted if used as a proxy for soil moisture where wildfires occur, such as on peatlands. Broadly, SAR intensity is correlated positively with soil moisture at Ballynafagh as expected, (Dobson et al., 1992). The average increase of SAR intensity observed after the wildfire, however, is clearly related to the removal of the mossy vegetation layer by wildfire. The SAR intensity increases in the burnt areas corresponds to the NDVI reduction there (Figure 2 e-f), which we attribute to fire-related vegetation removal (Figure 1 b-c). In support of this interpretation, we note that outside the SAC area containing the bog, similar reductions of NDVI can be seen also in fields within which grass or cereal crops were recently harvested (Figure 2 e-f). Intensity changes are therefore an integration of two layers on the peatlands (mossy and upper peat layers). Without accounting for effects of wildfire, SAR intensity potentially yields overestimations of soil moisture.

InSAR coherence has recently emerged as an alternative means of estimating soil moisture, (De Zan & Gomba, 2018; Zwieback et al., 2015b). The aim of InSAR coherence investigations are twofold: (1) to estimate soil moisture at a finer spatial resolution and (2) to correct InSAR-derived displacements, as proposed by Zwieback et al. (2017). However, estimating soil moisture from InSAR coherence and phase appears to be complex and statically unsustainable on conventional soils, (Eshqi Molan & Lu, 2020a). Our InSAR application on a peatland shows a good relationship between peat parameters and the InSAR parameters, which means that InSAR coherence could be an appropriate tool for organic soil moisture estimation in the case of relatively healthy raised peatlands. Moreover, our results demonstrate that InSAR coherence is not affected by changes to vegetation wrought by the early-July 2019 wildfire unlike SAR intensity, InSAR coherence could be more robust to estimate soil moisture on peatlands affected by wildfire.

4.4. Penetration of C-band radar beam into temperate raised peatland

The lack of effect of the 2019 wildfire on the InSAR coherence and displacement at Ballynafagh can be interpreted as evidence that the satellite-derived C-band radar waves penetrate into the upper several cm of the peat (Nolan & Fatland, 2003). From Figure 8 which shows a schematic interpretation, the propagation of radar beams is shown for the "pre-fire" and "post-fire" periods. Before the fire, the radar beam firstly penetrates thought the 10-20 cm thick mossy vegetation, attenuating backscatter intensity (approx. -3 to -2 dB). Then the radar waves continue to propagate into the upper few 10's of cm of the underlying peat, where the intensity further decreases and the radar phase (i.e., InSAR phase and coherence) is affected by changes in soil moisture. After the fire and without the 10-20 cm mossy vegetation layer, the intensity increases on average as the vegetation-related attenuation is reduced, but it varies in a positive relationship with the variation of soil moisture in the peat layer.

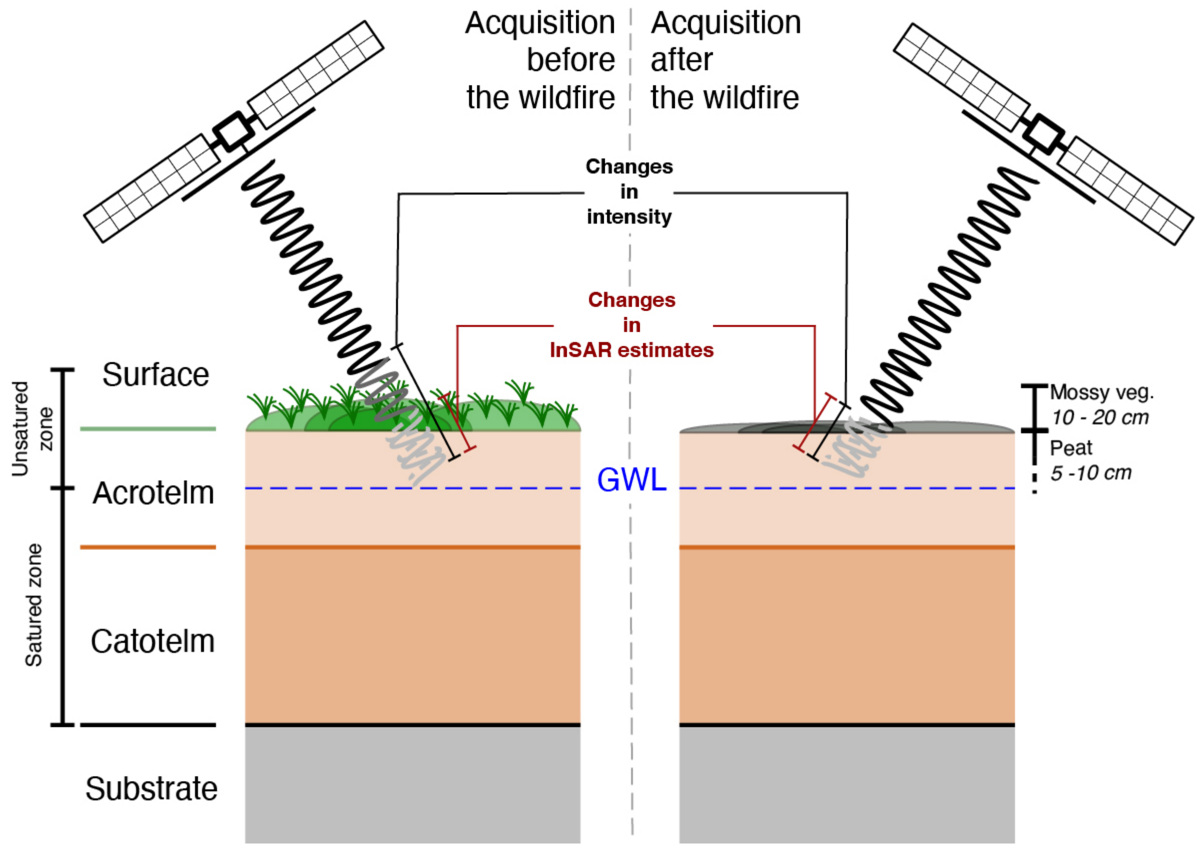

Figure 8: Schematic representation of InSAR propagation in peat associated with climatic controls on soil moisture changes, for active raised bog or healthy areas of bog.

In contrast. the InSAR phase and coherence are unaffected by the removal of the vegetation, although they also vary with soil moisture variation. In this case, we interpret that there is a decoupling of the SAR and InSAR measurements on the peatlands. This is because the intensity changes relate to the changes in both soil moisture and vegetation, whereas the InSAR estimates (phase) are not affected by the mossy layer. Therefore, the vegetation layer contributes negligibly to the medium (level) controlling the backscattered radar phase in this raised peatland. Consequently, the SAR and InSAR parameters represent the layers of the peatland.

5. Conclusions

In summary, our study explored the full range of InSAR products and their relationships to in-situ soil moisture and groundwater level measurements over a temperate peatland affected by a wildfire. We draw four main conclusions.

Firstly, the InSAR-estimated peat surface displacements display annual oscillations ("bog breathing") that are synchronous and positively correlated with the seasonal (dry/wet) evolutions of soil moisture and groundwater levels. Thus, peat surface displacements should be an indicator of short-term variations in ecohydrological parameters, such as groundwater levels.

Secondly, SAR intensity positively correlates with absolute values of soil moisture. Thus, SAR intensity oscillates on seasonal timeframes: it increases in wet periods and decreases in dry periods.

Thirdly, InSAR coherence negatively correlates with changes in soil moisture. Consequently, InSAR coherence is low for large soil moisture changes, and is high for small soil moisture changes between two SAR acquisitions. Moreover, the designing of InSAR stack should take into account the relationship to optimise the coherence of the InSAR stack, and avoid coherence loss due to sharp soil moisture changes especially across dry periods.

Fourth, the wildfire highlighted how SAR and InSAR estimates relate to different attributes for raised peatlands: (1) SAR intensity is affected by both changes in soil moisture and vegetation; (2) InSAR coherence is affected by only soil moisture changes. Consequently, SAR and InSAR data from C-band radar sensor reveal information on different levels in the peat column.

These findings can underpin the application and interpretation of radar in monitoring of peatland soil parameters in general and in areas affected by wildfires. Future work should therefore focus on ground validation of InSAR displacements from in-situ measurements in order to verify the accuracy of InSAR results and to identify the possible magnitude of bias caused by soil moisture on displacement observations.

Data availability

The additional figures can be found in the Supplementary Materials. All the InSAR products and scripts used to analyse the observations are available from the corresponding authors.

CRediT authorship contribution statement

Alexis Hrysiewicz: Conceptualisation, Data computation, Investigation and Analysis, Methodology, Visualisation, Writing – original draft. **Eoghan P. Holohan:** Project Funding and administration, Conceptualisation, Investigation and Analysis, Methodology, Visualisation, Writing – original draft, Supervision. **Shane Donohue:** Conceptualisation, in-situ data extraction, Investigation and Analysis. **Hugh Cashnan:** In-situ data extraction and Investigation.

Acknowledgments

The authors acknowledge support from Science Foundation Ireland (SFI), University College Dublin (UCD) and the SFI Research Centre In Applied Geosciences hosted by UCD (iCRAG-Phase 2 – Grand Code: 13/RC/2092_P2). The authors also thank John Walsh (UCD) for his support in setting up the InSAR lab at UCD and GAMMA staff for technical support. We acknowledge the European Space Agency (ESA) for the Sentinel-1 data and NASA for SRTM DEM.

Declaration of Competing Interest

The authors declare no competing interests.

References

Alshammari, L., Boyd, D. S., Sowter, A., Marshall, C., Andersen, R., Gilbert, P., Marsh, S., & Large, D. J. (2020). Use of Surface Motion Characteristics Determined by InSAR to Assess Peatland Condition. *Journal of Geophysical Research: Biogeosciences*, *125*(1), 1-15. https://doi.org/10.1029/2018JG004953

Alshammari, L., Large, D. J., Boyd, D. S., Sowter, A., Anderson, R., Andersen, R., & Marsh, S. (2018). Long-term peatland condition assessment via surface motion monitoring using the ISBAS DInSAR technique over the Flow Country, Scotland. *Remote Sensing*, *10*(7). https://doi.org/10.3390/rs10071103

Asmuß, T., Bechtold, M., & Tiemeyer, B. (2018). *Towards Monitoring Groundwater Table Depth in Peatlands from Sentinel-1 Radar Data* IGARSS 2018 - 2018 IEEE International Geoscience and Remote Sensing Symposium, Valencia, Spain.

Balenzano, Mattia, F., Satalino, Pauwels, & Snoeij. (2012). SMOSAR ALGORITHM FOR SOIL MOISTURE RETRIEVAL USING SENTINEL-1 DATA (1) Consiglio Nazionale delle Ricerche (CNR) – Istituto di Studi sui Sistemi Intelligenti per l ' Automazione (ISSIA), Bari , Italy (2) Ghent University – Laboratory of Hydrology a. (1), 1200-1203.

Balenzano, A., Mattia, F., Satalino, G., Lovergine, F. P., Palmisano, D., Peng, J., Marzahn, P., Wegmüller, U., Cartus, O., Dąbrowska-Zielińska, K., Musial, J. P., Davidson, M. W. J., Pauwels, V. R. N., Cosh, M. H., McNairn, H., Johnson, J. T., Walker, J. P., Yueh, S. H., Entekhabi, D., . . . Jackson, T. J. (2021). Sentinel-1 soil moisture at 1 km resolution: a validation study. *Remote Sensing of Environment*, *263*. https://doi.org/10.1016/j.rse.2021.112554

Barrett, B. (2012). The Use of C- and L-Band Repeat-Pass Interferometric SAR Coherence for Soil Moisture Change Detection in Vegetated Areas. *The Open Remote Sensing Journal*, *5*(1), 37-53. https://doi.org/10.2174/1875413901205010037

Bateson, L., Cigna, F., Boon, D., & Sowter, A. (2015). The application of the intermittent SBAS (ISBAS) InSAR method to the South Wales Coalfield, UK. *International Journal of Applied Earth Observation and Geoinformation*, *34*(1), 249-257. https://doi.org/10.1016/j.jag.2014.08.018

Bechtold, M., Schlaffer, S., Tiemeyer, B., & De Lannoy, G. (2018). Inferring Water Table Depth Dynamics from ENVISAT-ASAR C-Band Backscatter over a Range of Peatlands from Deeply-Drained to Natural Conditions. *Remote Sensing*, *10*(4). https://doi.org/10.3390/rs10040536

Casu, F., Manzo, M., & Lanari, R. (2006). A quantitative assessment of the SBAS algorithm performance for surface deformation retrieval from DInSAR data. *Remote Sensing of Environment*, *102*(3-4), 195-210. https://doi.org/10.1016/j.rse.2006.01.023

Cigna, F., Novellino, A., Jordan, C. J., Sowter, A., Ramondini, M., & Calcaterra, D. (2014). Intermittent SBAS (ISBAS) InSAR with COSMO-SkyMed X-band high resolution SAR data for landslide inventory mapping in Piana degli Albanesi (Italy). *SAR Image Analysis, Modeling, and Techniques XIV*, *9243*, 92431B-92431B. https://doi.org/10.1117/12.2067424

Cigna, F., Sowter, A., Jordan, C. J., & Rawlins, B. G. (2014). Intermittent Small Baseline Subset (ISBAS) monitoring of land covers unfavourable for conventional C-band InSAR: proof-of-concept for peatland environments in North Wales, UK. *SAR Image Analysis, Modeling, and Techniques XIV*, *9243*, 924305-924305. https://doi.org/10.1117/12.2067604

Connolly, J., & Holden, N. M. (2009). Mapping peat soils in Ireland: Updating the derived Irish peat map. *Irish Geography*, *42*(3), 343-352. https://doi.org/10.1080/00750770903407989

Connolly, J., Holden, N. M., & Ward, S. M. (2007). Mapping Peatlands in Ireland using a Rule-Based Methodology and Digital Data. *Soil Science Society of America Journal*, *71*(2), 492-499. https://doi.org/10.2136/sssaj2006.0033

Cross, J. (1990). *The raised bogs of Ireland: their ecology, status and conservation*. Stationery Office.

De Zan, F., & Gomba, G. (2018). Vegetation and soil moisture inversion from SAR closure phases: First experiments and results. *Remote Sensing of Environment*, *217*(2017), 562-572. https://doi.org/10.1016/j.rse.2018.08.034

De Zan, F., Parizzi, A., Prats-Iraola, P., & López-Dekker, P. (2014). A SAR interferometric model for soil moisture. *IEEE Transactions on Geoscience and Remote Sensing*, *52*(1), 418-425. https://doi.org/10.1109/TGRS.2013.2241069

De Zan, F., Zonno, M., & Lopez-Dekker, P. (2015). Phase Inconsistencies and Multiple Scattering in SAR Interferometry. *IEEE Transactions on Geoscience and Remote Sensing*, *53*(12), 6608-6616. https://doi.org/10.1109/TGRS.2015.2444431

Dobson, M. C., Pierce, L., Sarabandi, K., Ulaby, F. T., & Sharik, T. (1992). Preliminary analysis of ERS-1 SAR for forest ecosystem studies. *IEEE Transactions on Geoscience and Remote Sensing*, *30*(2), 203-211.

Drösler, M., Freibauer, A., Torben, C. R., & Friborg, T. (2008). Observations and status of peatland greenhouse gas emissions in Europe. In *The Continental-Scale Greenhouse Gas Balance of Europe* (pp. 243--261). Springer. https://doi.org/10.1007/978-0-387-76570-9

Eshqi Molan, Y., & Lu, Z. (2020a). Can InSAR Coherence and Closure Phase Be Used to Estimate Soil Moisture Changes? *Remote Sensing*, *12*(9). https://doi.org/10.3390/rs12091511

Eshqi Molan, Y., & Lu, Z. (2020b). Modeling InSAR Phase and SAR Intensity Changes Induced by Soil Moisture. *IEEE Transactions on Geoscience and Remote Sensing*, *58*(7), 4967-4975. https://doi.org/10.1109/tgrs.2020.2970841

Ewing, J. M., & Vepraskas, M. J. (2006). Estimating primary and secondary subsidence in an organic soil 15, 20, and 30 years after drainage. *Wetlands*, *26*(1), 119-130. https://doi.org/10.1672/0277-5212(2006)26[119:EPASSI]2.0.CO;2

Farr, T. G., Rosen, P. A., Caro, E., Crippen, R., Duren, R., Hensley, S., Kobrick, M., Paller, M., Rodriguez, E., Roth, L., Seal, D., Shaffer, S., Shimada, J., Umland, J., Werner, M., Oskin, M., Burbank, D., & Alsdorf, D. E. (2007). The shuttle radar topography mission. *Reviews of Geophysics*, *45*(2), RG2004-RG2004. https://doi.org/10.1029/2005RG000183

Fernandez, F., Connolly, K., Crowley, W., Deneyer, J., Duff, K., & Smith, G. (2014). *Raised Bog Monitoring and Assessment Survey 2013*.

Ferretti, A., Prati, C., & Rocca, F. (2001). Permanent scatterers in SAR interferometry. *IEEE Transactions on Geoscience and Remote Sensing*, *39*(1), 8-20. https://doi.org/10.1109/36.898661

Fiaschi, S., Holohan, E. P., Sheehy, M., & Floris, M. (2019). PS-InSAR Analysis of Sentinel-1 Data for Detecting Ground Motion in Temperate Oceanic Climate Zones: A Case Study in the Republic of Ireland. *Remote Sensing*, *11*(3). https://doi.org/ARTN 348

10.3390/rs11030348

Fritz, C., Campbell, D. I., & Schipper, L. A. (2008). Oscillating peat surface levels in a restiad peatland, New Zealand-magnitude and spatiotemporal variability. *Hydrological Processes*, *22*(17), 3264-3274. https://doi.org/10.1002/hyp.6912

Gorham, E. (1991). Northern Peatlands: Role in the Carbon Cycle and Probable Responses to Climatic Warming. *Ecol Appl*, *1*(2), 182-195. https://doi.org/10.2307/1941811

Heikurainen, L., Päivänen, J., & Sarasto, J. (1964). Ground water table and water content in peat soil.

Hiraishi, T., Krug, T., Tanabe, K., Srivastava, N., Baasansuren, J., Fukuda, M., & Troxler, T. (2014). 2013 supplement to the 2006 IPCC guidelines for national greenhouse gas inventories: Wetlands. *IPCC, Switzerland*.

Hooijer, A., Page, S., Canadell, J. G., Silvius, M., Kwadijk, J., Wösten, H., & Jauhiainen, J. (2010). Current and future CO 2 emissions from drained peatlands in Southeast Asia. *Biogeosciences*, *7*(5), 1505-1514. https://doi.org/10.5194/bg-7-1505-2010

Hooijer, A., Page, S., Navratil, P., Vernimmen, R., & Mawdsley, N. (2014). Carbon Emissions from Drained and Degraded Peatland in Indonesia and Emission Factors for Measurement , Reporting and Verification (MRV) of Peatland Greenhouse Gas Emissions. *Forda-Mof.Org*(May), 50-50. http://www.forda-mof.org/files/12._Carbon_Emissions_from_Drained_and_Degraded_Peatland_in_Indonesia.pdf

Hooper, A. J. (2008). A multi-temporal InSAR method incorporating both persistent scatterer and small baseline approaches. *Geophysical Research Letters*, *35*(16), L16302-L16302. https://doi.org/10.1029/2008GL034654

Howie, S. A., & Hebda, R. J. (2018). Bog surface oscillation (mire breathing): A useful measure in raised bog restoration. *Hydrological Processes*, *32*(11), 1518-1530. https://doi.org/10.1002/hyp.11622

Hoyt, A. M., Chaussard, E., Seppalainen, S. S., & Harvey, C. F. (2020). Widespread subsidence and carbon emissions across Southeast Asian peatlands. *Nature Geoscience*, *13*(6), 435-440. https://doi.org/10.1038/s41561-020-0575-4

Jones , K., Lanthier, Y., van der Voet, P., van Valkengoed, E., Taylor, D., & Fernandez-Prieto, D. (2009). Monitoring and assessment of wetlands using Earth Observation: The GlobWetland project. *Journal of Environmental Management 90*, 2154-2169. https://doi.org/10.1016/j.jenvman.20 07.07.037

Kelly, L. (1993). *Hydrology, Hydrochemistry and Vegetation of Two Raised Bogs in Co. Offaly* Ph. D. Thesis. Trinity College, Dublin. Available at: http://www. npws. ie …].

Kelly, L., & Schouten, M. G. C. (2002). Vegetation. In M. G. C. Schouten (Ed.), *Conservation and restoration of raised bogs: geological, hydrological and ecological studies* (pp. 110-169). The Heritage Service of the Department of the Environment and Local Government, Ireland; Staatsbosbeheer, the Netherlands; Geological Survey of Ireland, Dublin.

Kettridge, N., Thompson, D. K., & Waddington, J. M. (2012). Impact of wildfire on the thermal behavior of northern peatlands: Observations and model simulations. *Journal of Geophysical Research: Biogeosciences*, *117*(G2), n/a-n/a. https://doi.org/10.1029/2011jg001910

Khakim, M. Y. N., Bama, A. A., Yustian, I., Poerwono, P., Tsuji, T., & Matsuoka, T. (2020). Peatland subsidence and vegetation cover degradation as impacts of the 2015 El niño event revealed by Sentinel-1A SAR data. *International Journal of Applied Earth Observation and Geoinformation*, *84*. https://doi.org/10.1016/j.jag.2019.101953

Kim, J.-W., Lu, Z., Gutenberg, L., & Zhu, Z. (2017). Characterizing hydrologic changes of the Great Dismal Swamp using SAR/InSAR. *Remote Sensing of Environment*, *198*, 187-202. https://doi.org/10.1016/j.rse.2017.06.009

Köchy, M., Hiederer, R., & Freibauer, A. (2015). Global distribution of soil organic carbon – Part 1: Masses and frequency distributions of SOC stocks for the tropics, permafrost regions, wetlands, and the world. *Soil*, *1*(1), 351-365. https://doi.org/10.5194/soil-1-351-2015

Lees, K. J., Quaife, T., Artz, R. R. E., Khomik, M., & Clark, J. M. (2018). Potential for using remote sensing to estimate carbon fluxes across northern peatlands – A review. *Science of the Total Environment*, *615*, 857-874. https://doi.org/10.1016/j.scitotenv.2017.09.103

Leifeld, J., & Menichetti, L. (2018). The underappreciated potential of peatlands in global climate change mitigation strategies /704/47/4113 /704/106/47 article. *Nature Communications*, *9*(1). https://doi.org/10.1038/s41467-018-03406-6

Massonnet, D., & Feigl, K. L. (1998). Radar interferometry and its application to changes in the earth's surface. *Reviews of Geophysics*, *36*(4), 441-500. https://doi.org/10.1029/97RG03139

Millard, K., & Richardson, M. (2018). Quantifying the relative contributions of vegetation and soil moisture conditions to polarimetric C-Band SAR response in a temperate peatland. *Remote Sensing of Environment*, *206*(December 2017), 123-138. https://doi.org/10.1016/j.rse.2017.12.011

Millard, K., Thompson, D. K., Parisien, M. A., & Richardson, M. (2018). Soil moisture monitoring in a temperate peatland using multi-sensor remote sensing and linear mixed effects. *Remote Sensing*, *10*(6). https://doi.org/10.3390/rs10060903

Molan, Y. E., Lu, Z., & Kim, J.-W. (2020). Influence of the Statistical Properties of Phase and Intensity on Closure Phase. *IEEE Transactions on Geoscience and Remote Sensing*, *58*(10), 7346-7354. https://doi.org/10.1109/tgrs.2020.2982062

Nesti, G., Tarchi, D., & Rudant, J.-P. (1995). Decorrelation of backscattered signal due to soil moisture changes. IEEE International Symposium on Geoscience and Remote Sensing, Firenze, Italy.

Nolan, M., & Fatland, D. R. (2003). Penetration depth as a DInSAR observable and proxy for soil moisture. *IEEE Transactions on Geoscience and Remote Sensing*, *41*(3), 532-537. https://doi.org/10.1109/tgrs.2003.809931

Paloscia, S., Pettinato, S., Santi, E., Notarnicola, C., Pasolli, L., & Reppucci, A. (2013). Soil moisture mapping using Sentinel-1 images: Algorithm and preliminary validation. *Remote Sensing of Environment*, *134*, 234-248. https://doi.org/10.1016/j.rse.2013.02.027

Parish, F., Sirin, A., Charman, D., Joosten, H., Minayeva, T., Silvius, M., & Stringer, L. (2008). *Assessment on Peatlands, Biodiversity and Climate Change: Main Report. Global Environment Centre, Kuala Lumpur and Wetlands International, Wageningen*.

Peng, J., Albergel, C., Balenzano, A., Brocca, L., Cartus, O., Cosh, M. H., Crow, W. T., Dabrowska-Zielinska, K., Dadson, S., Davidson, M. W. J., de Rosnay, P., Dorigo, W., Gruber, A., Hagemann, S., Hirschi, M., Kerr, Y. H., Lovergine, F., Mahecha, M. D., Marzahn, P., . . . Loew, A. (2021). A roadmap for high-resolution satellite soil moisture applications – confronting product characteristics with user requirements. *Remote Sensing of Environment*, *252*. https://doi.org/10.1016/j.rse.2020.112162

Reddy, A. D., Hawbaker, T. J., Wurster, F., Zhu, Z., Ward, S., Newcomb, D., & Murray, R. (2015). Quantifying soil carbon loss and uncertainty from a peatland wildfire using multi-temporal LiDAR. *Remote Sensing of Environment*, *170*, 306-316. https://doi.org/10.1016/j.rse.2015.09.017

Regan, S., Flynn, R., Gill, L., Naughton, O., & Johnston, P. (2019). Impacts of Groundwater Drainage on Peatland Subsidence and Its Ecological Implications on an Atlantic Raised Bog. *Water Resources Research*, *55*(7), 6153-6168. https://doi.org/10.1029/2019WR024937

Renou-Wilson, F., Moser, G., Fallon, D., Farrell, C. A., Müller, C., & Wilson, D. (2019). Rewetting degraded peatlands for climate and biodiversity benefits: Results from two raised bogs. *Ecological Engineering*, *127*, 547-560. https://doi.org/10.1016/j.ecoleng.2018.02.014

Roulet, N. T. (2000). Peatlands, carbon storage, greenhouse gases, and the kyoto protocol: Prospects and significance for Canada. *Wetlands*, *20*(4), 605-615. https://doi.org/10.1672/0277-5212(2000)020[0605:PCSGGA]2.0.CO;2

Scheiber, R., & Moreira, A. (2000). Coregistration of interferometric SAR images using spectral diversity. *IEEE Transactions on Geoscience and Remote Sensing*, *38*(5), 2179-2191. https://doi.org/10.1109/36.868876

Sowter, A., Bateson, L., Strange, P., Ambrose, K., & Fifiksyafiudin, M. (2013). Dinsar estimation of land motion using intermittent coherence with application to the south derbyshire and leicestershire coalfields. *Remote Sensing Letters*, *4*(10), 979-987. https://doi.org/10.1080/2150704X.2013.823673

Takada, M., Mishima, Y., & Natsume, S. (2009). Estimation of surface soil properties in peatland using ALOS/PALSAR. *Landscape and Ecological Engineering*, *5*(1), 45-58. https://doi.org/10.1007/s11355-008-0061-4

Tampuu, T., Praks, J., Uiboupin, R., & Kull, A. (2020). Long Term Interferometric Temporal Coherence and DInSAR Phase in Northern Peatlands. *Remote Sensing*, *12*(10). https://doi.org/10.3390/rs12101566

Wagner, W., Sabel, D., Doubkova, M., Bartsch, A., & Pathe, C. (2013). the Potential of Sentinel-1 for Monitoring Soil Moisture With a High Spatial Resolution At Global Scale. *Cycle*, *2009*(November 2009), 18-20.

Wegmüller, U., Werner, C., Strozzi, T., Wiesmann, A., Frey, O., & Santoro, M. (2015). Sentinel-1 IWS mode support in the GAMMA software. 2015 IEEE 5th Asia-Pacific Conference on Synthetic Aperture Radar (APSAR),

Wegnüller, U., Werner, C., Strozzi, T., Wiesmann, A., Frey, O., & Santoro, M. (2016). Sentinel-1 Support in the GAMMA Software. *Procedia Computer Science*, *100*, 1305-1312. https://doi.org/10.1016/j.procs.2016.09.246

Werner, C., Wegmüller, U., Strozzi, T., & Wiesmann, A. (2003). Interferometric point target analysis for deformation mapping. IGARSS 2003. 2003 IEEE International Geoscience and Remote Sensing Symposium.,

Wilkinson, S. L., Tekatch, A. M., Markle, C. E., Moore, P. A., & Waddington, J. M. (2020). Shallow peat is most vulnerable to high peat burn severity during wildfire. *Environmental Research Letters*, *15*(10). https://doi.org/10.1088/1748-9326/aba7e8

Xu, J., Morris, P. J., Liu, J., & Holden, J. (2018). PEATMAP: Refining estimates of global peatland distribution based on a meta-analysis. *Catena*, *160*, 134-140.

Yu, Z., Loisel, J., Brosseau, D. P., Beilman, D. W., & Hunt, S. J. (2010). Global peatland dynamics since the Last Glacial Maximum. *Geophysical Research Letters*, *37*(13), n/a-n/a. https://doi.org/10.1029/2010gl043584

Zebker, H. A., & Villasenor, J. (1992). Decorrelation in Interferometric Radar Echoes. *IEEE Transactions on Geoscience and Remote Sensing*, *30*(5), 950-959. https://doi.org/Doi 10.1109/36.175330

Zhang, T., Zeng, Q., Li, Y., & Xiang, Y. (2008). *Study on relation between InSAR coherence and soil moisture* XXIst ISPRS Congress Technical Commission VI, Beijing, China.

Zhou, Z. (2013). *The applications of InSAR time series analysis for monitoring long-term surface change in peatlands*

Zhou, Z., Li, Z., Waldron, S., & Tanaka, A. (2016). Monitoring peat subsidence and carbon emission in Indonesia peatlands using InSAR time series. *International Geoscience and Remote Sensing Symposium (IGARSS)*, *2016-November*, 6797-6798. https://doi.org/10.1109/IGARSS.2016.7730774

Zhou, Z., Waldron, S., & Li, Z. (2010). Integration of PS-InSAR and GPS for monitoring seasonal and long-term peatland surface fluctuations. Remote Sensing and the Carbon Cycle,

Zwieback, S., Hensley, S., & Hajnsek, I. (2015a). Assessment of soil moisture effects on L-band radar interferometry. *Remote Sensing of Environment*, *164*, 77-89. https://doi.org/10.1016/j.rse.2015.04.012

Zwieback, S., Hensley, S., & Hajnsek, I. (2015b). A Polarimetric First-Order Model of Soil Moisture Effects on the DInSAR Coherence. *Remote Sensing*, *7*(6), 7571-7596. https://doi.org/10.3390/rs70607571

Zwieback, S., Hensley, S., & Hajnsek, I. (2017). Soil Moisture Estimation Using Differential Radar Interferometry: Toward Separating Soil Moisture and Displacements. *IEEE Transactions on Geoscience and Remote Sensing*, *55*(9), 5069-5083. https://doi.org/10.1109/tgrs.2017.2702099